Available online at www.sciencedirect.com

SCIENCE DIRECT

Materials Letters 59 (2005) 1195–1199

materials letters

www.elsevier.com/locate/matlet

Densification and electrical conductivity of fast fired manganese-doped ceria ceramics

G.J. Pereira[a], R.H.R. Castro[a], D.Z. de Florio[b], E.N.S. Muccillo[c], D. Gouvêa[a,*]

[a]*Departamento de Engenharia Metalúrgica e de Materiais, Escola Politécnica, Universidade de S. Paulo, Av. Prof. Mello Moraes, 2463, S. Paulo, 05508-900, SP, Brazil*

[b]*Instituto de Química, UNESP, R. Prof. Francisco Degni s/n, Araraquara, 14801-970, SP, Brazil*

[c]*Centro Multidisciplinar para o Desenvolvimento de Materiais Cerâmicos, Instituto de Pesquisas Energéticas e Nucleares-CCTM, C.P. 11049, S. Paulo, 05422-970, SP, Brazil*

Received 22 May 2004; received in revised form 29 November 2004; accepted 12 December 2004
Available online 29 December 2004

Abstract

Reactive pure and manganese-doped (5% and 10 at.%) ceria nanosized powders were prepared by the polymeric precursor technique. Physical properties of powder materials were studied by X-ray diffraction, nitrogen adsorption, and diffuse reflectance infrared Fourier transform spectroscopy. Characterization of powder compacts after fast firing at 1200 °C for 5 min was carried out by scanning electron microscopy and impedance spectroscopy measurements. The bulk apparent density of sintered pellets was determined for pellets of different compositions sintered at 1200 °C. A gradual decrease of the particle size occurs with increasing doping content. Relatively high values of apparent density were obtained after fast firing doped specimens at 1200 °C. DRIFT spectra evidence that a fraction of Mn ions was segregated onto particles surface. The electrical resistivity of sintered pellets reveals different mechanisms of conduction depending on the Mn content.

Keywords: CeO_2; DRIFT; Fast firing; Electrical properties; Electroceramics; Impedance spectroscopy

1. Introduction

Cerium oxide either pure or doped has potentially a wide range of applications including gas sensors, catalytic supports for automobile exhaust systems, and electrode or electrolyte materials for solid oxide fuel cells [1–5].

Commercially available CeO_2 powders are difficult to sinter to high densities due to the high refractivity and undesirable characteristics related to severe agglomeration and large crystallite size. In addition, ceria exhibits a strong tendency to undergo reduction at high temperatures when a release of a gaseous phase was reported to retard densification [6].

The main approaches found in the literature to reduce the sintering temperature are the use of nanozised powder particles, and the introduction of additives [7–13]. The former is expected to provide faster densification kinetics and lower sintering temperatures, as predicted by Herring's scaling law [14]. The later is believed to produce the same effect by the creation of defects, which increase the kinetics of mass transport, or by changing the predominant mechanism to a liquid phase sintering.

The effect of manganese doping on sintering and densification of commercial ceria powder has been recently studied [12,13,15,16]. It was shown that doping ceria with manganese allowed a substantial reduction of the sintering temperature and enhanced the grain growth process.

In this work, the effects of Mn ions on surface and microstructural characteristics of nanosized ceria powders were studied by diffuse reflectance infrared Fourier transform spectroscopy (DRIFT), nitrogen adsorption, and X-ray diffraction (XRD) experiments. The microstructure and electrical conductivity of sintered specimens were verified

* Corresponding author. Tel.: +55 11 30915238; fax: +55 11 30915421.
E-mail address: dgouvea@usp.br (D. Gouvêa).

0167-577X/$ - see front matter © 2005 Elsevier B.V. All rights reserved.
doi:10.1016/j.matlet.2004.12.027

by scanning electron microscopy (SEM) and impedance spectroscopy, respectively.

2. Experimental procedure

Pure and manganese-doped cerium dioxide powders were prepared by a modified polymeric precursor method [17]. Nominal manganese contents were 5 and 10 at.%.

Cerium nitrate hexahydrate (99.9%, Aldrich) was dissolved into a 50 wt.% ethylene glycol (Synth, PA) and 30 wt.% citric acid (Synth, PA) solution under stirring. Increase of the temperature up to 110 °C resulted in the polyesterification reaction. For the synthesis of doped powders, suitable amounts of manganese (II) carbonate (99.9%, Alfa Aesar) were directly mixed to the precursor solution. The resulting resin was thermally decomposed at 450 °C for 4 h, homogenized in an agate mortar and calcined at 500 °C for 15 h. Further details of the method of synthesis may be found elsewhere [18].

Powder materials were uniaxially pressed into pellets with 6 mm of diameter and 2 mm thickness, at 392 MPa without any binder material. In order to verify the influence of the additive in controlling the driving force for sintering, the fast firing process, which is known to provide equivalent densities at smaller grain sizes in a less energy consuming process [19], was used. Green pellets were introduced into a pre-heated tubular furnace at 1200 °C. After 3 or 5 min of isothermal treatment, pellets were pulled out of the furnace and quickly cooled down to room temperature. For comparison purposes, a set of compacts was sintered at 1200 °C for 4 h.

Characterization of powder materials was carried out by X-ray diffraction (D8 Advance, Bruker-AXS) using a Cu K_α source in the 20° to 80° 2θ range for phase analysis. Values of specific surface area, S_{BET}, were determined from nitrogen adsorption (Gemini III 2375, Micromeritics) experiments using the Brunauer, Emmett and Teller (BET) method. Chemical groups on the surface of calcined powders were analyzed by diffuse reflectance infrared Fourier transform (Magna IR560, Nicolet) in the 400 to 4000 cm^{-1} wavenumber range.

The apparent density of sintered pellets was determined by measuring the sample weight and dimensions. Fractured surfaces were observed by scanning electron microscopy (Stereoscan 440, Leica Cambridge). Electrical conductivity of pellets was evaluated by impedance spectroscopy measurements (4192A, Hewlett Packard) in the 5 Hz to 13 MHz frequency range, in air. Data were analyzed in the impedance mode using a special computer program [20]. Resistance measurements were carried out in controlled oxygen pressures in the range 0.21 to ~10^{-6} atm. The different oxygen pressures were achieved by gas mixtures of oxygen and argon. Isobaric resistance measurements were carried out from ~300 to ~500 °C. Results of electrical measurements are plotted as the imaginary ($-Z''$) versus the real (Z') part of the impedance, normalized for sample dimensions. No corrections for specimens porosity was carried out.

3. Results and discussion

Fig. 1 shows X-ray diffraction patterns of pure (a) and manganese-doped ceria (b and c) calcined powders. The diffraction profile of nominally pure ceria (Fig. 1a) exhibits a characteristic fluorite-type lattice indexed according to ICDD-34-394. Diffraction patterns of doped-ceria powders (Fig. 1b and c) are similar to that of the pure material, without any diffraction peak that could be assigned to isolated manganese oxide or to any spurious phase. This result suggests that Mn ions enter into solid solution in the cubic fluorite lattice.

It is worth to note in Fig. 1 a gradual enlargement of all diffraction peaks with increasing dopant content. In general, line broadening of XRD patterns is a consequence of reduction in the crystallite (or primary particle) size. This effect was first observed in specimens prepared by the oxalate coprecipitation [21].

Values of specific surface area of calcined powders are shown in Table 1. There is an increase of the S_{BET} value or a decrease in the particle size with increasing the dopant content. This result agrees with that of XRD shown in Fig. 1. One possible explanation for this effect is that Mn ions incorporated into the cubic lattice reduce the rate of crystal growth in ceria particles.

Fig. 2 shows DRIFT spectra of pure and doped calcined ceria powders. In the low wavenumber range (Fig. 2b) several absorption bands are detected. These absorption bands are attributed to OH vibrations, and they change with doping. The intensity of the absorption band at 1350 cm^{-1} decreases and that at 1307 cm^{-1} increases with increasing dopant content, while vibrations at 1060 and 1040 cm^{-1}

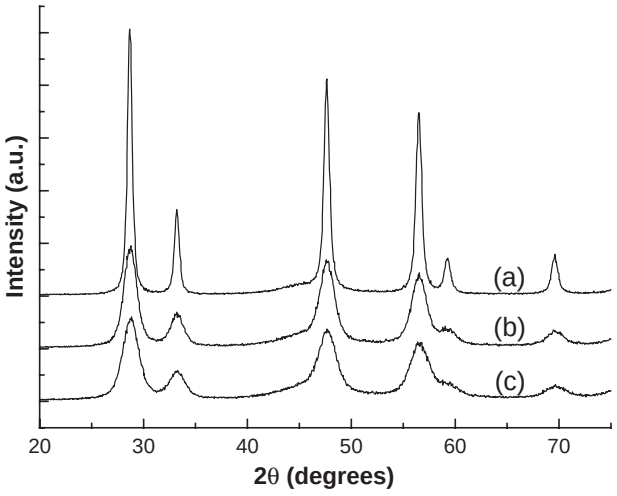

Fig. 1. XRD patterns of CeO_2 powders containing (a) 0%, (b) 5%, and (c) 10 at.% Mn.

Table 1
Values of S_{BET} of calcined pure and doped CeO_2 powders

Sample	S_{BET} (m^2 g^{-1})
CeO_2	11.7
5 at.% Mn	64.1
10 at.% Mn	82.0

experience a displacement in the wavenumber at the maximum amplitude. The DRIFT spectra at high wavenumbers (Fig. 2a) exhibit a prominent absorption band at 3690 cm^{-1}, which is assigned to the stretching of a OH group bound to Mn [22]. This result evidences that a fraction of Mn ions coexists with OH surface groups in calcined powders. Therefore, it appears that not all manganese ions enter into solid solution in ceria lattice, but remain segregated onto particle surfaces. It is known that cation segregation may occur even when there is solubility, and that these segregated cations may reduce the surface energy of the particles [23]. A similar effect was observed to occur in Mn- and Fe-doped SnO_2 [24,25].

The densification behavior of powder compacts with doping content is shown in Fig. 3. Nominally pure ceria compacts exhibit a limited densification after firing at 1200 °C, even for a holding time of 4 h. The relative density of doped compacts reaches ~90% 65 of the theoretical value with only 3 and 5 min of holding time at that temperature, showing that during sintering the effect of Mn doping CeO_2 is to increase the kinetics of densification. Increasing the holding time to 4 h results in a further increase in the relative density of doped pellet. In general, ceria either pure or doped is sintered at higher temperatures (>1500 °C) to obtain a high densification [6]. The relatively high densification of doped ceria may be attributed to both phenomena: the creation of oxygen vacancies as charge compensating defects due to solid solution formation, and the decrease of

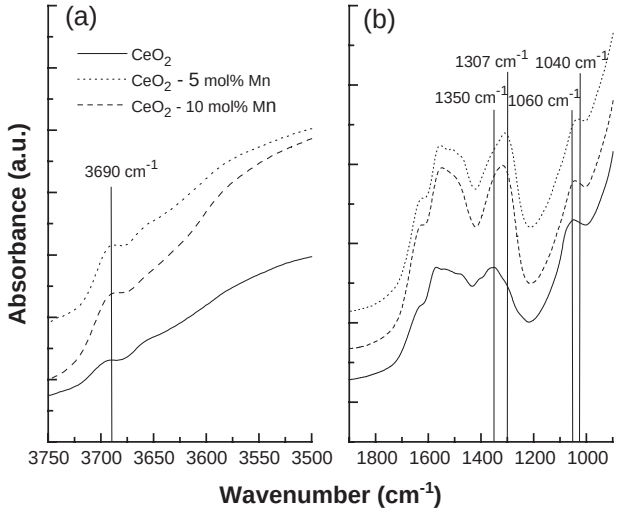

Fig. 2. DRIFT spectra of pure and Mn-doped CeO_2 powders.

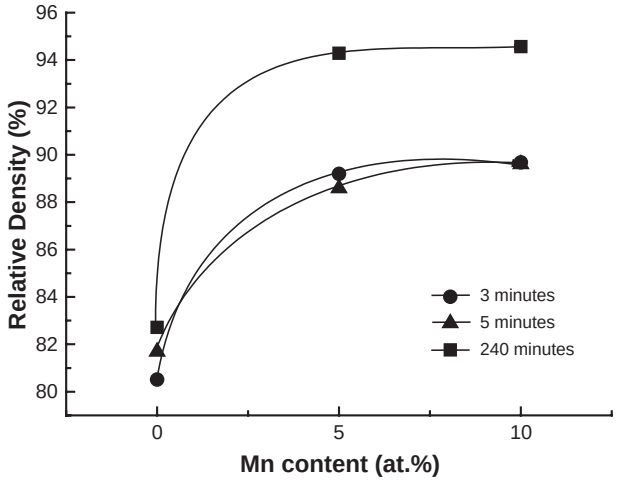

Fig. 3. Relative density of sintered pellets with different Mn contents.

interface (solid–solid and solid–gas) energies due to dopant segregation [26].

Representative SEM micrographs of fracture surfaces of sintered compacts are shown in Fig. 4.

The main microstructure features for pure ceria are a relatively high porosity and small grain size compared with doped specimens. This result agrees with that observed in commercial ceria doped with manganese [15]. It is known from the literature that transition metal oxides act as sintering aid to ceria compounds. Small additions of CoO (up to 1 mol%), for example, allowed the densification of gadolinia-doped ceria ceramics at temperatures as low as 900 °C with reduced grain growth [13]. Comparing these microstructure features with those shown in the literature [13], it can be concluded, however, that transition metal oxide additions may have a different effect concerning the grain growth process, although all of them contribute at some extent to densification of ceria ceramics.

Fig. 5 shows impedance diagrams in air at 435 °C obtained for sintered specimens of pure and manganese-doped ceria.

The impedance diagrams of sintered pellets exhibit two well-resolved semicircles in the frequency range of measurements. The high-frequency semicircle is due to capacitive and resistive effects of the bulk of pellets, whereas the low-frequency semicircle is usually attributed to the blocking of charge carriers at interfaces. The specimen of pure ceria is highly resistive and the whole impedance diagram is seen only at higher measuring temperatures. However, the bulk resistivity, related to the high-frequency semicircle, is quite low compared to that of doped specimens. It is known from the literature that blocking of charge carriers at interfaces may occur due to defects of either extrinsic (impurities and secondary phases) or intrinsic (pores and cracks) origin, and is responsible for the increase of the total ceramic resistivity [27,28]. The impedance result for pure ceria agrees with the microstructure features (relatively low grain size and high fraction of porosity) observed in Fig. 4.

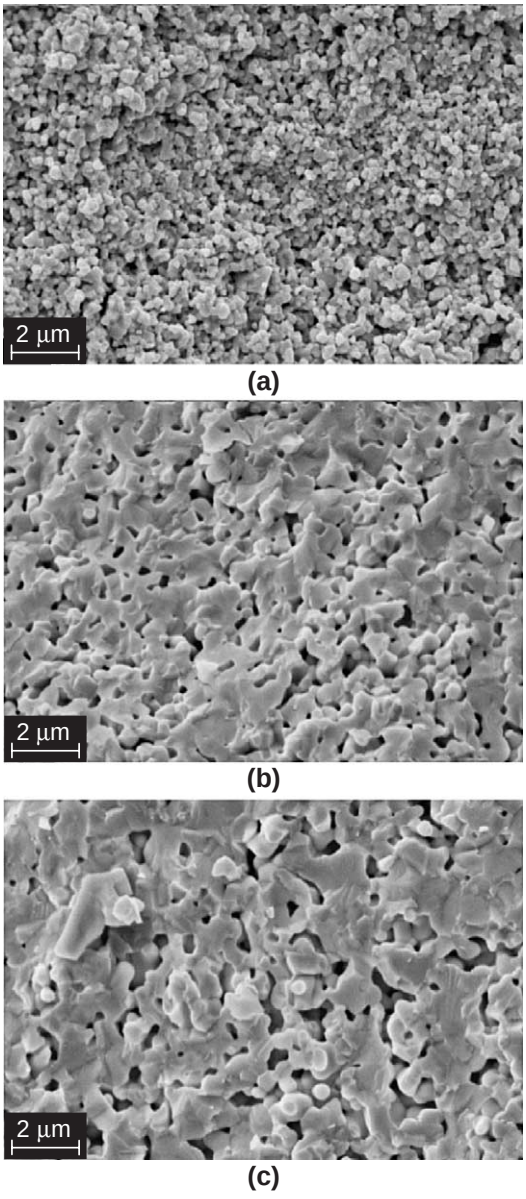

Fig. 4. SEM micrographs of (a) CeO_2, and CeO_2 pellets doped with Mn (b) 5% and (c) 10% sintered at 1200 °C for 3 min.

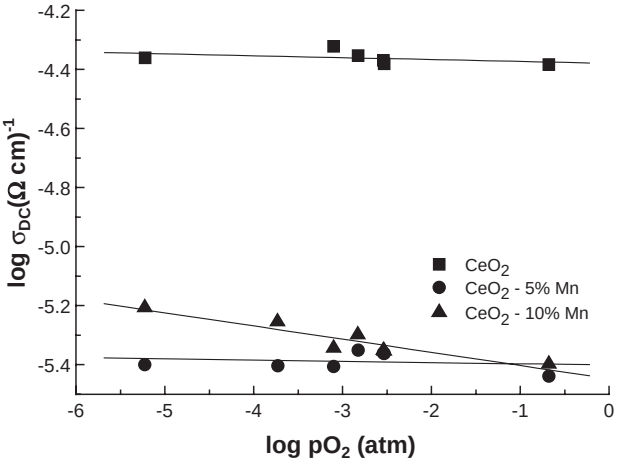

Fig. 6. Conductivity versus oxygen partial pressure of sintered (holding time=3 min) CeO_2 pellets. Electrode material: Pt.

The bulk resistivity of ceria ceramics initially increases with doping with manganese ions, and then beyond a specific content (≥5 at.%) of additive, it decreases. These changes in the bulk resistivity is an additional evidence of the solid solution formation between cerium and manganese oxides. Values of apparent activation energy for conduction determined from Arrhenius plots of electrical resistivity resulted in 0.74 and 0.67 eV for ceria doped with 5 and 10 at.% Mn, respectively.

The blocking contribution to the total resistivity is greatly reduced with Mn doping. This result demonstrates that not all manganese ions are in the bulk of the material.

Fig. 6 shows the bulk (pure CeO_2) and the total (doped CeO_2) electrical conductivity versus oxygen partial pressure of pellets sintered at 1200 °C for 3 min. The electrical conductivities of pure and CeO_2—5 at.% Mn do not depend on the oxygen partial pressure, indicating a predominant ionic conduction behavior. In contrast, the pellet containing 10 at.% Mn seems to exhibit a small *p*-type conductivity. However, the observed variation is too small to obey classical power laws.

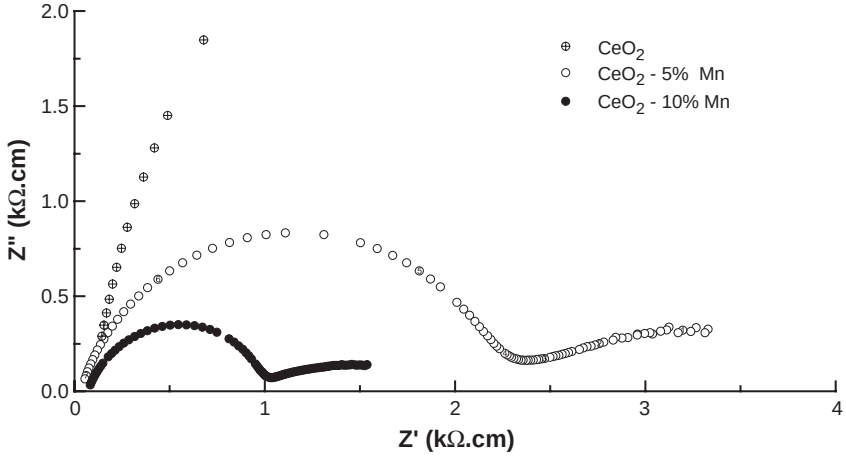

Fig. 5. Impedance spectroscopy diagrams at 435 °C in air of sintered (holding time=3 min) CeO_2 pellets. Electrode material: Ag.

Impedance results shown here refer to specimens sintered at 1200 °C for 3 min. Results of other ceria ceramics sintered at different temperatures and holding times, and a full analysis of the conduction properties and densification behavior will be the subject of a forthcoming paper.

4. Conclusions

Doping of ceria with manganese ions produced a gradual decrease of the particle size of calcined powders. A relatively high densification of powder compacts was obtained after firing at 1200 °C, even for short holding times. Impedance spectroscopy measurements give further evidence that Mn ions enter into solid solution and increase the electrical conductivity by reducing the apparent activation energy. In addition, DRIFT result shows that a fraction of manganese ions remains segregated onto particles surface. This segregation effect may also be responsible for the high densification attained by sintered pellets. Higher manganese contents introduce an electronic conduction behavior in ceria ceramics.

Acknowledgements

To FAPESP (96/09604-9, 99/04929-5, 99/10798-0, and 01/10053-7), CNPq (300934/94-7), CAPES, and CNEN for financial supports.

References

[1] T. Kudo, H. Obayashi, J. Electrochem. Soc. 122 (1975) 42.
[2] H. Yahiro, Y. Baba, K. Eguchi, H. Arai, J. Electrochem. Soc. 135 (1988) 2077.
[3] P. Fornasiero, G. Balducci, R.D. Monte, J. Kaspar, V. Sergo, G. Gubitosa, A. Ferrero, M. Graziani, J. Catal. 164 (1996) 173.
[4] A. Trovarelli, C. deLeitenburg, G. Dolcetti, Chemtech 27 (1997) 32.
[5] T. Hibino, A. Hashimoto, T. Inoue, J. Tokuno, S. Yoshida, M. Sano, Science 288 (2000) 2031.
[6] Y.C. Zhou, M.N. Rahaman, Acta Mater. 45 (1997) 3635.
[7] P.-L. Chen, I.-W. Chen, J. Am. Ceram. Soc. 76 (1993) 1577.
[8] Y.C. Zhou, M.N. Rahaman, J. Mater. Res. 8 (1993) 1680.
[9] T. Suzuki, P.G. McCormick, J. Am. Ceram. Soc. 84 (2001) 1453.
[10] J.F. Baumard, C. Gault, A. Argoitia, J. Less-Common Met. 127 (1987) 125.
[11] Z. Tianshu, P. Hing, H. Huang, J. Kilner, J. Mater. Process. Technol. 113 (2001) 463.
[12] Z. Tianshu, P. Hing, H. Huang, J. Kilner, Mater. Lett. 57 (2002) 507.
[13] C. Kleinlogel, L.J. Gauckler, Adv. Mater. 13 (2001) 1081.
[14] C. Herring, J. Appl. Phys. 21 (1950) 301.
[15] Z. Tianshu, P. Hing, H. Huang, J. Kilner, Mater. Sci. Eng. B83 (2001) 235.
[16] C.M. Kleinlogel, L.J. Gauckler, J. Electroceram. 5 (2000) 231.
[17] M.P. Pechini, US Patent 3,330,697 (1967).
[18] D. Gouvêa, R.L. Villalobos, J.D.T. Capocchi, Mat. Sci. Forum 299 (1999) 91.
[19] D.E. Garcia, J. Seidel, R. Janssen, N. Claussen, J. Eur. Ceram. Soc. 15 (1995) 935.
[20] M. Kleitz, J.H. Kennedy, in: P. Vashishta, J.N. Mundy, G.K. Shenoy (Eds.), Fast Ion Transport in Solids, Electrodes and Electrolytes, North-Holland, Amsterdam, 1979.
[21] A.E.C. Palmqvist, M. Wirde, U. Gelius, M. Muhammed, NanoStruct. Mater. 11 (1999) 995.
[22] M. Richtera, A. Trunschke, U. Bentrup, K.W. Brzezinka, E. Schreier, M. Schneider, M.M. Pohl, R. Fricke, J. Catal. 206 (2002) 98.
[23] S.H. Overbury, P.A. Bertrand, G.A. Somorjai, Chem. Rev. 75 (1975) 547.
[24] W.C. Las, D. Gouvea, W. Sano, Solid State Sci. 1 (1999) 331.
[25] G.J. Pereira, R.H.R. Castro, P. Hidalgo, D. Gouvea, Appl. Surf. Sci. 195 (2002) 277.
[26] D. Gouvea, R.H.R. Castro, Appl. Surf. Sci. 217 (2003) 194.
[27] L. Dessemond, R. Muccillo, M. Hénault, M. Kleitz, Appl. Phys., A 57 (1993) 57.
[28] E.N.S. Muccillo, M. Kleitz, J. Eur. Ceram. Soc. 16 (1996) 453.